Driving Experience and Behavior Change in Remote Driving

An Explorative Experimental Study

Zhao, Lin; Nybacka, Mikael; Rothhamel, Malte; Habibovic, Azra; Papaioannou, Georgios; Drugge, Lars

DOI
10.1109/TIV.2023.3344890

Publication date
2024

Document Version
Final published version

Published in
IEEE Transactions on Intelligent Vehicles

Driving Experience and Behavior Change in Remote Driving: An Explorative Experimental Study

Lin Zhao, Mikael Nybacka, Malte Rothhämel, Azra Habibovic, Georgios Papaioannou, and Lars Drugge

***Abstract*—Remote driving plays an essential role in coordinating automated vehicles in some challenging situations. Due to the changed driving environment, the experiences and behaviors of remote drivers would undergo some changes compared to conventional drivers. To study this, a continuous real-life and remote driving experiment is conducted under different driving conditions. In addition, the effect of steering force feedback (SFF) on the driving experience is also investigated. In order to achieve this, three types of SFF modes are compared. According to the results, no SFF significantly worsens the driving experience in both remote and real-life driving. Additionally, less force and returnability on steering wheel are needed in remote driving, and the steering force amplitude appears to influence the steering velocity of remote drivers. Furthermore, there is an increase in lane following deviation during remote driving. Remote drivers are also prone to driving at lower speeds and have a higher steering reversal rate. They also give larger steering angle inputs when crossing the cones in a slalom manoeuvre and cause the car to experience larger lateral acceleration. These findings provide indications on how to design SFF and how driving behavior and experience change in remote driving.**

***Index Terms*—Remote driving, driving behavior, driving experience, driving performance, steering force feedback.**

I. Introduction

REMOTE driving has drawn significant attention since it is widely considered a backup system for automated vehicles (AVs) allowing the smooth and safe transition to fully AVs [1]. Currently, AVs still pose many challenges and can encounter difficulties to operate in a fully automated mode in various situations [2]. For example, AVs might struggle in new city areas, since high-precision maps may not be updated in a timely manner, and road markings and signs may be missing. In addition, extreme weather and poor situational awareness as well as changing environments, such as demonstrations or sports events, will pose challenges for AVs [3]. For this reason, and to accelerate the commercialisation of AVs, remote driving has been developed for their control in challenging scenarios or when they are not allowed to operate due to legal issues.

Although many startups [4], [5], [6] and universities [7], [8] have begun exploring various aspects of remote driving, there are still many challenges to address such as situational awareness [9], [10], [11] and latency [12], [13], [14]. Many efforts have been made to overcome the above challenges, such as enhancing situational awareness through video improvements and reducing latency through predictive algorithms. To improve situational awareness with visual assistance during remote driving, separate techniques have been developed to assist drivers in locating vehicles [15], and recognising speed [11] and distance [16]. Meanwhile, vehicle state [8], [17], [18] and video prediction methods [19], [20] have been implemented to overcome the latency in remote driving.

However, only a limited number of studies have thoroughly investigated the impact of remote driving on driving experience and behavior, despite the relevance of these factors during driving. Papaioannou et al. [21] discovered a significant increase in motion sickness levels among passengers during remote driving compared to real-life driving. This effect is attributed to the heightened steering velocity in remote driving scenarios. Similarly, Zhao et al. [22] found that remote driving resulted in higher workload demands compared to real-life driving. While these studies offer valuable insights into the changes in driving behavior and experience in remote driving, there remains a gap in the literature regarding a comprehensive exploration of detailed changes, such as driving accuracy, and lateral and longitudinal driving behaviors.

Furthermore, few related works consider enriching the driving experience by bringing remote drivers into the loop and providing kinematic feedback. Such methods could include incorporating steering force and motion-cueing feedback into the remote driving station (RDS). These methods are important human-machine-interaction (HMI) channels for driving. For example, drivers can use motion-cueing and steering force feedback (SFF) to assess driving conditions such as road surfaces, tyre-road force, and vehicle motion. Nevertheless, these are still blank areas in remote driving, and this work paves the way for their proper development.

Manuscript received 10 October 2023; revised 24 November 2023; accepted 10 December 2023. Date of publication 20 December 2023; date of current version 29 April 2024. This work was supported by the REDO FFI Project under Grant 2019-03068, is vital and made by Vinnova. *(Corresponding author: Lin Zhao.)*

This work involved human subjects or animals in its research. Approval of all ethical and experimental procedures and protocols was granted by Swedish Ethical Review Authority under Application No. 2020-05020.

Lin Zhao, Mikael Nybacka, Malte Rothhämel, and Lars Drugge are with the Department of Engineering Mechanics, KTH Royal Institute of Technology, 11428 Stockholm, Sweden (e-mail: linzhao@kth.se; mnybacka@kth.se; m2rotmal@kth.se; larsd@kth.se).

Azra Habibovic is with Scania CV AB, S-15187 Södertälje, Sweden (e-mail: azra.habibovic@scania.com).

Georgios Papaioannou is with Cognitive Robotics Department, Delft University of Technology, 2628, CD Delft, The Netherlands (e-mail: g.papaioannou@tudelft.nl).

Color versions of one or more figures in this article are available at https://doi.org/10.1109/TIV.2023.3344890.

Digital Object Identifier 10.1109/TIV.2023.3344890

TABLE I
STEERING FORCE FEEDBACK MODEL COMPARISON

Method	Main principle	Advantages	Disadvantages
Torque-map based SFF [23, 24].	Using collected offline data to map the correlation between vehicle states and steering feedback force.	(1). Stable and concise. (2). The influence of delay can be decreased.	(1). Large dataset is needed for various scenarios. (2). Hard to simulate the detailed road disturbance force.
Machine learning based SFF [25, 26].	Using the real car's data to train the SFF model.	Nonlinear characteristics of SFF can be better represented.	(1). Large dataset is needed. (2). Low robust performance for untrained scenarios.
Physical model based SFF [27].	Using mathematic model to represent the physical characteristics of steering system.	(1). With high fidelity. (2). It is easy to tune the parameter and to be applied.	Large parameter uncertainty.
Adaptive SFF model [28].	The adaptive observers are used to overcome parameter uncertainties in steering system.	The effect of parameter uncertainty will be decreased.	Algorithm complexity will be greatly increased and hard to be applied.
Modular model based SFF [22].	Using steering motor current as main input to reflect the tyre-road forces to steering wheel.	(1). It can feedback realistic SFF, such as road disturbances. (2). Less parameters need to be tuned.	It is easy to disturb remote drivers unless filtered.

SFF plays a crucial role in influencing driving performance and experience, as demonstrated by driving simulator studies [29], [30]. The Steer-by-Wire (SbW) system in the conventional car shares similarities with the steering system in remote driving. Consequently, classical SFF models employed in SbW might find utility in remote driving. SbW can employ diverse SFF models, encompassing the torque-map based, machine learning based, physical, adaptive, and modular models, as presented in Table I. It shows the advantages and disadvantages of the performance of each model from different aspects. For the torque-map based model [23], [24], it is stable, concise and has the possibility to reduce the impact of delay, but it needs a large dataset that covers various scenarios as much as possible, which greatly increases the application difficulty. It is also difficult to simulate the detailed effect of road disturbance using this model. The machine learning based SFF model [25], [26] has some similarities in that it also requires a large dataset to train the model, which accounts for the low robustness performance when applied to scenarios beyond its training scope. For the physical model based SFF (PF) [27], it has high fidelity and is easy to apply, but there is the possibility of a large uncertainty of the parameters. The adaptive SFF model [28] can reduce the impact of parameter uncertainty, but the complexity of the algorithm increases greatly and makes it difficult to apply in a real application. The modular model based SFF (MF) [22] can feedback drivers with realistic feeling, including detailed road disturbance feel, since it uses the steering motor current as the main force. It is simple to apply, since only few parameters need to be tuned. However, drivers may be disturbed by unwanted disturbances in the feedback.

The realistic driving experience in remote driving is important. Therefore, MF and PF are adopted in this experiment, since MF can provide realistic feedback to drivers and PF has high fidelity. For the disadvantages of MF, a proper filter can be applied to remove unnecessary signals. For PF, validated parameters from the literature can be used to overcome the disadvantage of parameter uncertainty. In addition, for establishing a baseline, a No steering force Feedback (NF) setting is also incorporated. These three variables constitute the experimental framework. Furthermore, a seamless comparative test is conducted between real-life and remote driving to examine how the driving behavior and experience change.

The main research aims (RAs) in this study is outlined as follows:

RA 1: Study drivers' adaptation to the driving environment in remote driving.
RA 2: Study the changes in the steering force feedback requirements during remote driving.
RA 3: Study the changes in driving experience and how different SFF models influence it in remote driving.
RA 4: Study the changes in driving behavior and performance in remote driving.
RA 5: Perform correlation studies between driving experience and behavior.

The current paper is an extension of authors' published conference paper [22]. In the conference paper, the authors studied: (1) the SFF requirements for remote driving and the impact of different SFF models on driving behavior and experience; (2) the changes in mental workload during remote driving; (3) the process by which drivers adapt to the driving environment and scenarios during both remote and real-life driving. The results from these studies provide the initial conclusions for *RAs 1-2*, while an introductory analysis for *RA 3* is presented in the conference paper without any statistical comparison between remote and real-life driving. This work delves into these topics in more detail. Regarding *RA 3* more specifically, this work utilises the *t-test* to assess the significance of the changes in driving experience between remote and real-life driving, while also analysing how different SFF models affect driving experience in both driving environments. Additionally, this paper provides a broader analysis through the use of multiple metrics from different dimensions to achieve *RAs 4-5*, on which the conference paper does not focus at all. Furthermore, this paper also provides a detailed explanation of how the remote driving is set up, including specific information on the sources of components, suppliers, and possible problems in remote driving and methods to handle them. Furthermore, the survey results pertaining to the remote drivers' driving experience are also included in order to provide additional knowledge to this research area.

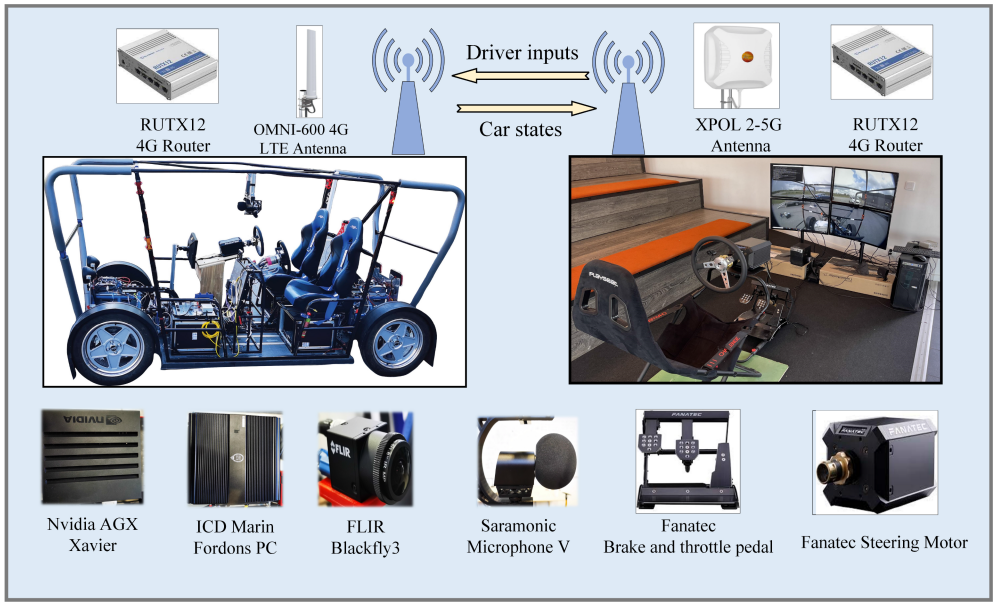

Fig. 1. Remote driving platform [22], which shows the RDV (left) and RDS (right). The components associated with remote driving are shown at the top and bottom.

The layout of this article is outlined as follows: Section II illustrates the hardware set-up for remote driving. The modelling process of SFF models is shown in Section III. Section IV details the experimental design, while the results and conclusions from the experiment are presented in Sections V and VI, respectively.

II. Remote Driving Set-Up

This section provides detailed information of the settings of the remote driving platform used in the experiment. According to Fig. 1, the hardware set-up mainly includes two parts: the remote driving vehicle[1] (RDV) and remote driving station (RDS). In the RDV, two FLIR[2] cameras are used to collect high-resolution real-world video. In addition, a Saramonic microphone[3] is mounted in the middle position to collect stereo audio for remote drivers.

For signal transmission between the RDV and RDS, an AGX Xavier[4] computer is first used to process the video; then, the OdenVR software provided by Voysys[5] is used to perform video encoding and decoding. The software can also provide multiple-link capability, which can automatically connect to other 4G signals if the current signal is too weak to support remote driving. This is, however, not implemented in this experiment due to a lack of time. Furthermore, video transmission is sometimes terminated when a commercial 4G router is used that does not have an external antenna in the pre-test, especially during the cornering manoeuvre; this might be due to the wrong relative direction between the 4G base station and the router. This signal is stabilised by using the RUTX12[6] router and OMNI-600,[7] a vertical column antenna, to avoid the directional issue. This provided a stable 4G signal even during the cornering manoeuvre. Similarly, an XPOL-5G[8] antenna with a square shape is used with the RDS since a stronger signal can be provided when it faces the base station. Finally, the Voysys-supplied latency measurement equipment is used to measure the glass-to-glass latency, which is kept close to 120 ms.

In the RDS, four low latency (4 ms) Samsung monitors[9] are used to provide video information. For steering force feedback, the same Fanatec kit[10] (DD2 steering motor and ClubSport V3 pedals) is used in both the RDV and RDS to reduce the hardware impact on the driving experience. The mathematical model is implemented in the vehicle's central controller (dSpace MicroAutobox II[11]), and an ICD Marin Fordons computer[12] is used to collect vehicle information and control the vehicle's Fanatec kit. The UDP communication method is used to transmit signals among vehicle controllers (e.g., AGX computer and dSpace controller).

III. Steering Force Feedback Modelling

This section provides the modelling process of SFF. In addition to the NF setting, two different SFF models (PF and

[1][Online]. Available: https://www.itrl.kth.se/research/completed-projects/research-concept-vehicle-model-e-1.917925
[2][Online]. Available: https://www.flir.com/products/blackfly-s-usb3/.
[3][Online]. Available: https://www.saramonic.com/about-us.
[4][Online]. Available: https://www.nvidia.com/en-us/autonomous-machines/embedded-systems/jetson-agx-xavier/.
[5][Online]. Available: https://www.voysys.se/.
[6][Online]. Available: https://teltonika-networks.com/.
[7][Online]. Available: https://poynting.tech/antennas/omni-600/.
[8][Online]. Available: https://poynting.tech/antennas/xpol-2-5 g/.
[9][Online]. Available: https://www.samsung.com/ie/business/business-monitors/curved-lc27f390fhuxen/.
[10][Online]. Available: https://fanatec.com/eu-en.
[11][Online]. Available: https://www.dspace.com/en/inc/home.cfm.
[12][Online]. Available: https://www.icd.se/produkt/icd-marin-fordons-pc-small-intel-i3-kaby-lake-240gb-ssd-4g/.

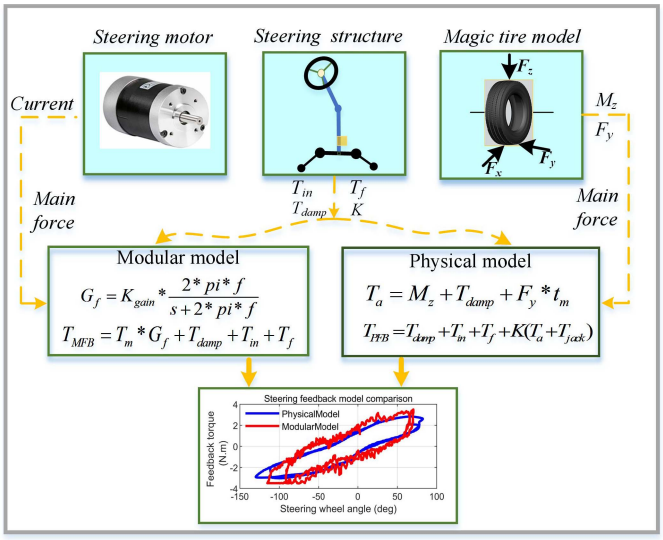

Fig. 2. Overall structure of MF (left) and PF (right), adapted from [22].

MF) are used to provide drivers with a total of three different driving experiences. The PF could provide smooth steering force feedback to the steering wheel. For the MF, it provides, apart from the traditional steering feedback force, a real-world feeling of disturbances, such as vibrations on gravel road surfaces. The model structures and the output comparison are shown in Fig. 2. Before the main experiment, several preliminary tests are conducted to calibrate and test the steering force feedback models. Some experienced drivers from the vehicle dynamic domain participate in these tests to calibrate and validate the SFF models.

A. Modular Model

The primary input of MF comes from the current of steering motor to obtain actual information about the tire-road interaction. In order to replicate the dynamic characteristics of the steering system, the corresponding dynamic relating to steering damping and inertia are simulated [31].

1) Main Torque: Within the modular framework, the main force is ascertained by the current value of the steering motor. It can represent the force between the tire and the road under various conditions [32]. Any alteration of the current value is directly linked to the change in the steering rack force, which can represent the lateral force between the tire and road. Additionally, the motor current contains high-frequency road data, comprising vibrations induced by disturbances such as speed-bumps and gravel, thus contributing further significant information to the steering wheel.

In order to provide drivers with appropriate steering feedback force, it is necessary to scale the current value to provide drivers with a good level of feedback based on what they reported in pre-tests before the experiment. This relationship is represented mathematically as

$$\tau_m = K_I * I \tag{1}$$

where τ_m represents the main torque, which relies on the current value (I) and is modulated by the current's gain (K_I). The K_I value, set at 0.0015 for this study, is ascertained considering both the driver's preferences and the actual current value. Furthermore, taking into account the vehicle's condition and the reference spectrum offered by [33], the upper limit of the feedback torque is modified to 3.5 Nm.

A bi-level control strategy based on frequency and amplitude is implemented to enable drivers to perceive the type of road through SFF. A cut-off bandpass filter is used to provide remote drivers with road signals of varying amplitude and frequency, depending on the road surface being concrete or gravel. The transfer function for this bi-level filter is defined as

$$G_s = K_s * \frac{2 * pi * f}{s + 2 * pi * f} \tag{2}$$

where K_s signifies the gain used to scale the amplitude corresponding to diverse road types. As illustrated in [34], it can be used to help drivers distinguishing the type of road by varying the scaling factors of amplitude control. In standard driving scenarios, the scaling factor K_s is definded as 1, and for gravel terrains, it is 4, a determination grounded on real testing experiences and the suggestions presented in [34]. Regarding frequency control, the study by Chen et al. [35] indicate that frequencies beneath 1 Hz encompass valuable low-frequency road feedback, especially at vehicle speeds under 20 km/h. The studies further emphasize the importance of stochastic road feedback like that from cobblestone surfaces, which occurs between 1 Hz and 30 Hz. The investigation also discloses that signal frequencies above 10 Hz induce considerable disturbances. In this research, a cut-off frequency of 1 Hz is adopted for standard concrete roads, and 10 Hz for gravel terrains, aiming to convey more precise road feeling to drivers.

2) Damping Torque: In the conventional steering system, the damping torque is generated by mechanical transmission. To emulate these intrinsic characteristics within a remote driving environment, the following equation is used to simulate the damping torque.

$$\tau_{damp} = C_{damp} * \dot{\delta}_{sw} \tag{3}$$

where τ_{damp} denotes the damping torque and C_{damp} represents a tunable parameter, set to 0.0262 $\mathrm{Nm/rad.s^{-1}}$. It is determined based on the suggested range outlined in [27]. The symbol $\dot{\delta}_{sw}$ represents the velocity of steering wheel.

3) Inertia Torque: To enhance the realism of the steering wheel feedback, an adjustable inertia parameter is employed to generate the inertia torque using a transfer function in this study. The transfer function is given by

$$G_{in} = \frac{J_s s}{1 + t_{filt} s} \tag{4}$$

where J_s denotes the inertia constant, assigned a value of 0.0017 $\mathrm{kg.m^2}$. t_{filt} is the filter parameter, which is set as 0.01. Both parameters align with the recommendations in [27], [31]. Subsequently, the inertia torque, denoted as τ_{in}, is formulated as follows:

$$\tau_{in} = G_{in} * \dot{\delta}_{sw} \tag{5}$$

4) Friction Torque: To minimize unnecessary motion in the steering wheel, the Coulomb friction are employed to simulate the feedback torque, following the methodology outlined in [31]. The torque in question is formulated as follows

$$\tau_f = K_s \cdot \tanh(h_s \cdot \dot{\delta}_{sw}) \tag{6}$$

where τ_f signifies the friction torque. K_s represents the peak value, which is established at 1 Nm. The variable h_s acts as a determinant factor influencing the friction torque, assigned a value of 0.05 in the present study, ascertained in accordance with the range outlined in [31]. Finally, the modular model based SFF can be experessed as:

$$\tau_{MFB} = \tau_m \cdot G_s + \tau_{damp} + \tau_{in} + \tau_f \tag{7}$$

where τ_{MFB} denotes the SFF of the modular model.

B. Physical Model

The aligning and jacking torques, originating from the tire forces simulated by the magic formula tire model, are integrated within the physical model. Furthermore, this model utilizes damping, inertia, and friction torque, computed in (3), (5), and (6) respectively, inherent in the steering system. The foundational structure of this model is based on references [27] and [36], details of which will be elaborated in the following sections.

1) Aligning and Jacking Torque: The main source of the steering wheel's aligning torque stems from the aligning moment and the jacking torque. These quantities can be described using the Pacejka's magic formula tire model [37] as

$$F_y = D_y \cdot \sin(C_y \cdot \arctan(B_y \cdot \alpha) - E_y \cdot (B_y \cdot \alpha - \arctan(B_y \cdot \alpha))) + S_{vy} \tag{8}$$

$$M_z = D_z \cdot \sin(C_z \cdot \arctan(B_z \cdot \alpha) - E_z \cdot (B_z \cdot \alpha - \arctan(B_z \cdot \alpha))) + S_{vz} \tag{9}$$

The parameters associated with the tire are obtained from the ADAMS/Tire software, as indicated in [38]. The tire slip angle, denoted as α, is approximated by employing the nonlinear dynamic state function [27]. The calculation of the aligning moment is represented as τ_a

$$\tau_a = M_z + F_y \cdot d_m \tag{10}$$

where τ_a denotes the aligning torque of the tire, and d_m is the mechanical trail intrinsic to the vehicle's design. Variations in the vertical forces exerted by the tires lead to the generation of jacking torque. As delineated in [39], this form of torque is mathematically described as a spring model and is represented by the following equation

$$\tau_{jack} = -K_j \cdot \theta_{rw} \tag{11}$$

where K_j signifies the spring stiffness, which is set the same as in reference [27]. In addition, the angle of the road wheel is denoted by θ_{rw}.

2) Steering Feedback Force: The force feedback relayed to the operators should include the inertia, damping, and torque originating from the column and rack. These specific torques align with those incorporated in the modular model, as shown in (3), (5), and (6). Similar with the modular model, the steering feedback force in the physical model can be represented as

$$\tau_{PFB} = \tau_{damp} + \tau_{in} + \tau_f + K_t(\tau_a + \tau_{jack}) \tag{12}$$

where τ_{PFB} signifies the feedback force originating from the physical model, whereas K_t stands for the coefficient transferring the torques from tire to drivers. To maintain the feedback force of both the physical and modular models within an identical range, the coefficient K_t is empirically assigned a value of 0.008, determined through preliminary tests with multiple participants.

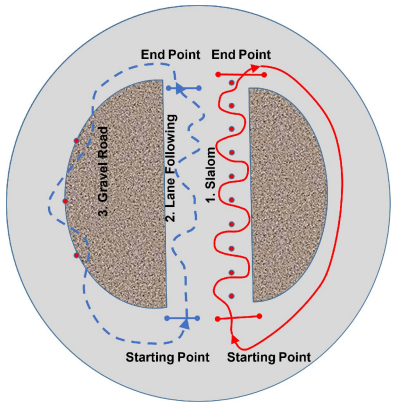

Fig. 3. Test scenarios, to the left the lane following and gravel road and to the right the slalom track [22].

IV. Experimental Design

A. Scenario Design

To further explore the driving experience and behavior in remote driving, this study employs two distinct scenarios (Fig. 3). The first is a slalom scenario with a distance of 15 m between each cone. The second scenario is the own-designed lane following scenario, consisting of a lane with changing curvature to be followed by the drivers. The curvature in the initial 40 m is relatively minor and straightforward to navigate, contrasting with the following 40 m, where drivers encounter frequent alterations in direction and curvature magnitude, increasing the task's complexity. This variation implies that drivers are likely to encounter heightened challenges and potentially experience increased steering feedback force in the lane-following task. Participants are told to track the lane with the front-left wheel and, subsequently, navigate a gravel road to experience real-world vibrations via the steering wheel. The order in which drivers tested the steering feedback models is changed during the test, but the order of scenarios is kept the same for real-life and remote driving.

Experimental results show that the average time required to complete the slalom and lane following scenarios in real-life driving are 19.19 seconds (SD = 1.38) and 21.33 seconds (SD = 2.35), respectively, which are lower than the average time in remote driving, which are 19.68 seconds (SD = 2.41) and 22.12 seconds (SD = 3.35).

TABLE II
SUBJECTIVE ASSESSMENT QUESTIONNAIRE [22]

Level 1	Level 2	Level 3
SA0. Overall assessment 0 1 2 3 4 5 Bad (0) → Neutral → Good(5)	SA10. Safety assessment 0 1 2 3 4 5 Unsafe (0) → Neutral → Safe(5)	SA11. Steering feedback support to control the vehicle through scenario: 0 1 2 3 4 5 Little support (0) → Neutral → High support(5) SA12 Steering feedback communication of the vehicle behaviour: 0 1 2 3 4 5 Bad (0) → Neutral → Good(5)
	SA20. Steering wheel characteristic feel 0 1 2 3 4 5 Unrealistic (0) → Neutral → Realistic(5)	SA21. Level of feedback force: 0 1 2 3 4 5 Too small (0) → Neutral → Too large(5) SA22. Returnability of steering wheel to centre: 0 1 2 3 4 5 Too slow (0) → Neutral → Too quick(5)
	SA30. Confidence and control 0 1 2 3 4 5 Unconfident (0) → Neutral → Confident(5)	SA31. Your assessment of the degree of success of accomplishing the task is: 0 1 2 3 4 5 Failure (0) → Neutral → Success(5) SA32 Your assessment of the difficulty of accomplishing the task is: 0 1 2 3 4 5 Easy (0) → Neutral → Difficult(5)
	SA40. Real world feel 0 1 2 3 4 5 Unrealistic (0) → Neutral → Realistic(5)	SA41. Your assessment of the road disturbance during driving communication is: 0 1 2 3 4 5 Bad (0) → Neutral → Good(5) SA42. How realistic is the steering feedback: 0 1 2 3 4 5 Unrealistic (0) → Neutral → Realistic(5)

B. Questionnaire Design

In order to investigate the participants' driving experience, a comprehensive subjective assessment questionnaire encompassing diverse themes is formulated (Table II). The foundational concepts for designing this questionnaire are inspired by [40], while several enhancements, including the real-world feel and multilevel assessment, are integrated to adapt it for remote driving and could help achieve the research aims in this study.

The questionnaire used three levels of questions ranging from general to detailed, asking the drivers about their feel regarding the driving experience and steering feedback. For each question, a 0–5 scale is used with a step size of 0.25 as presented in Table II.

C. Experimental Protocol

Experiments are conducted with drivers performing the same tasks in real-life and remote driving. To quickly switch between real-life and remote driving, the RDS is assembled and configured at the test track office, which is about 100 m away from where the real-life driving take place. To help participants familiarise themselves with the experimental vehicle and realistic driving scenarios, they conduct the real-life driving first, immediately followed by the remote driving.

Before the experiment, participants will shut the eyes for two minutes to facilitate relaxation as well as stabilizing their heart rate. Subsequently, they practice the scenario for four laps to familiarize themselves with it. The SFF models distributed to the drivers for the practice session differed, with two participants using only the NF, two using only the PF, and one using only the MF. This variation aimed at reducing the impact of drivers' adaption to specific SFF models on the subjective and objective assessment of the subsequent formal test. In the formal test, three distinct feedback settings are utilized by the drivers, specifically, PF, MF, and NF. To mitigate the impact on driving experience due to the order of these settings, the sequence of steering feedback modes is varied among participants. The slalom scenario is tested first, with participants being told to keep the car as close as possible to the cones when passing them and to feel the steering force feedback. They are also told to drive as quickly as they feel comfortable with and to perform well in this scenario. In the lane-following scenario, the task allocated to participants is to keep the front-left tire on the lane marked by yellow tape. The

remainder of the protocol mirrors that of the slalom scenario. On the gravel road, the drivers are asked to focus on the feeling of the steering wheel vibrations.

In the intervals between each testing scenario, participants are allocated a 30 second rest period with eyes shut to facilitate relaxation. Following the completion of the slalom scenario, they begin the lane-following scenario, adhering to an identical test procedure and protocol. The methodology for remote driving is consistently applied. To obtain immediate insights into the drivers' perception of the steering feedback, participants are prompted to respond to the questionnnaire immediately when finishing each scenario. For safety purposes, the maximum speed during the experiment is limited to 18 km/h.

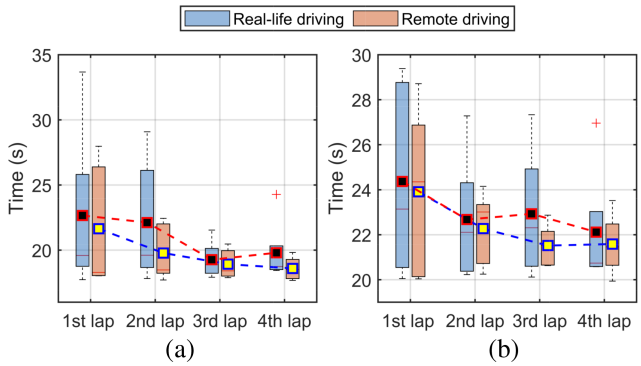

Fig. 4. Lap times during practice. (a) Slalom manoeuvre. (b) Lane following manoeuvre.

D. Participant Information

In this experiment, three people take part in the first day and two in the second. There is a six-day gap between the two days due to the availability of the test track. Each scenario, in both real-life driving and remote driving, encompassed a total of 15 cases, indicating that five drivers test three SFF modes. All participants have a passenger car driving license. The average age of them is 29.6 years, with a standard deviation of 8.56.

E. Survey With Participants

To explore the impact and requirements of remote driving and SFF across a broad range, a survey is conducted following the completion of the entire experiment. This methodology enabled participants to extensively delineate their experiences throughout the remote driving. Four survey themes are explored in this survey, which are summarized as follows: (a). Primary variances in steering feedback between remote and real-life driving; (b). Feedback characteristics that are essential to enhance driving performance; (c). The needed enhancements of steering feedback in remote driving; (d). Primary challenges in remote driving in comparison to real-life driving.

In order to give drivers enough time to reflect on these themes, they are asked to write down their answers on the paper without any time limit instead of giving verbal feedback.

V. Results Analysis and Discussion

To compare driving behavior and experience between remote and real-life driving, subjective and objective assessment methods are used separately. More specifically:

1) The lap time during practice is analysed to assess how drivers get used to the vehicle and the scenarios.
2) The driving experience, which includes the steering characteristics and feeling of safety, is evaluated using the subjective assessment.
3) The metrics for assessing driving behavior and performance during remote driving (i.e., throttle reversal rate) are considered and compared with real-life driving. The data between the 10th and 90th percentiles are used for the driving behavior comparison between remote and real-life driving in order to reduce the influence of outliers [41].
4) A linear regression analysis is performed to study the correlation between driving behavior and experience.

Boxplots are used to present the results of certain metrics, as shown in Fig. 4, where the black and yellow squares represent the mean values. A dashed line connects the points to represent the overall change in mean values. The median value is designated by a central red mark, whereas the red marker "+" signifies the identified outliers.

A. Learning Rate

The lap times for completing each manoeuvre are recorded for both scenarios during practice, which reflect drivers' familiarity with the scenario and the vehicle. According to Fig. 4(a), the time required to complete the manoeuvre from the first lap to the fourth lap gradually decreases. For real-life driving, the mean lap time drops approximately 8.7%, i.e., from 24.2 seconds for the first lap to 22.1 seconds for the fourth lap. Additionally, the data gradually becomes less scattered. Similarly to real-life driving, the mean lap time decreases from 23.9 seconds for the first lap to 21.6 seconds for the fourth lap during remote driving, indicating that drivers gradually get used to the manoeuvres. Furthermore, in both scenarios, the mean difference between the third and fourth lap is less than 4%, which is a small variance (approximately 1 second) in lap time for each manoeuvre. This implies that the drivers have already gotten used to the vehicle and the scenario from the third lap. In the lane following manoeuvre (Fig. 4(b)), the lap times are similar to those for the slalom.

Other metrics like velocity and throttle engagement also demonstrate the participants' learning process, and the difference between the last two laps is also small. In-depth details are available in [22].

B. Driving Experience Assessment

In this section, driving experience is analysed based on the subjective assessment (Table II) and the survey results. First, the overall assessment in Level 1 will be analysed; then, the results of the Level 2 and 3 questions will be provided. The subjective assessment during the slalom and lane following manoeuvres are combined for analysis to obtain more comprehensive results. Therefore, each box in the boxplots of Fig. 5 represents 10 data

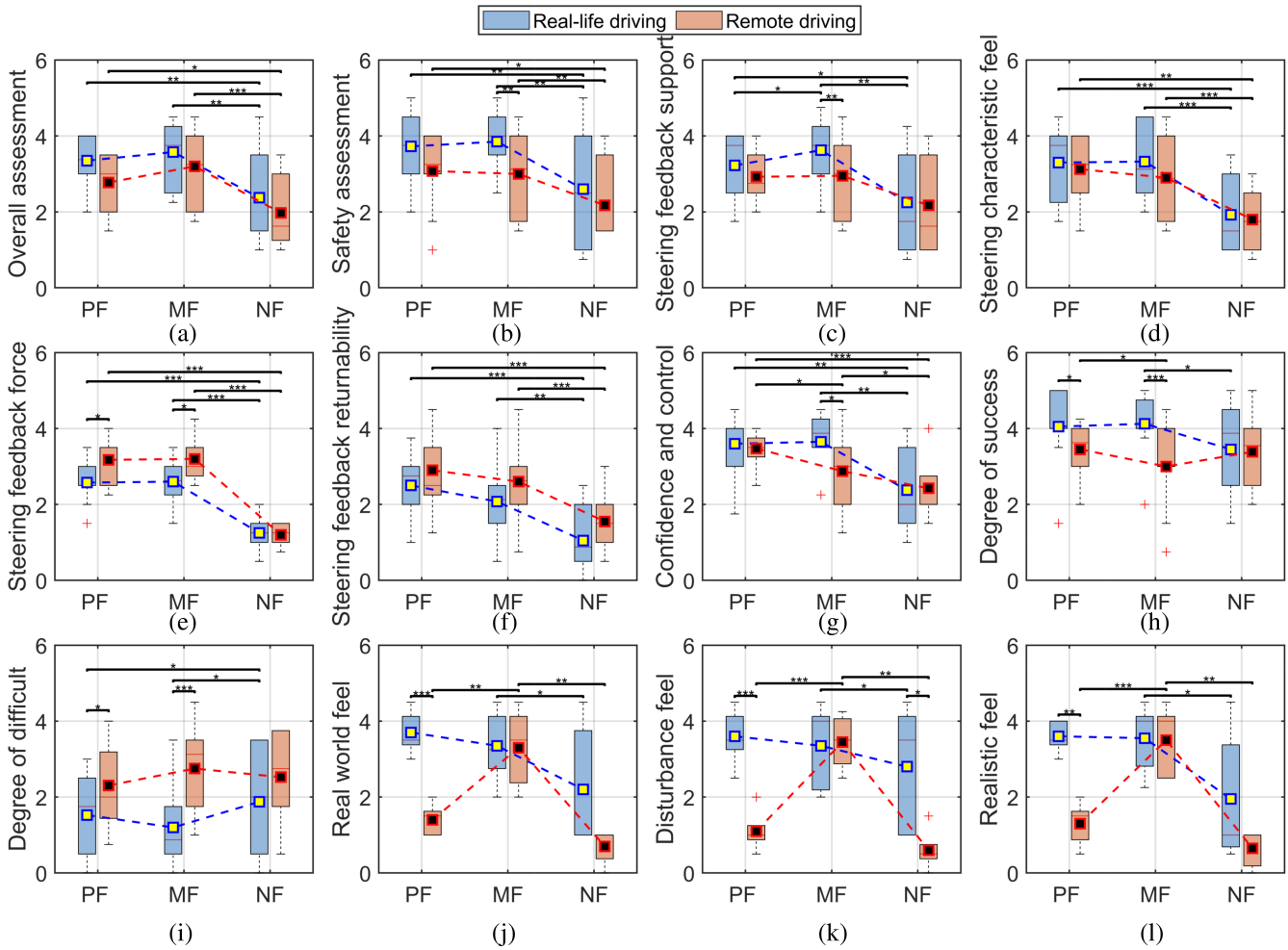

Fig. 5. Subjective assessment results regarding (a) SA 0 (Overall Assessment); (b) SA 10 (Safety Assessment); (c) SA 11 (Steering feedback support); (d) SA 20 (Steering characteristic feel); (e) SA 21 (Steering feedback force); (f) SA 22 (Steering feedback returnability); (g) SA 30 (Confidence and control); (h) SA 31 (Success feel); (i) SA 32 (Difficulty feel); (j) SA 40 (Real world feel); (k) SA 41 (Disturbance assessment); (l) SA 42 (Realistic assessment). The significance of paired t-test is denoted as $^{*}p \leq 0.05$, $^{**}p \leq 0.01$, and $^{***}p \leq 0.001$.

points (i.e., 5 drivers per SFF for 2 driving scenarios). The control variables in this figure include the different SFFs, i.e., PF, MF, and NF.

1) Overall Assessment: Fig. 5(a) shows the results of the overall assessment (SA 0). Similar trends between real-life and remote driving appear, wherein drivers assigned lower scores to NF compared to PF and MF ($p < 0.05$), as expected. When comparing MF and PF, it is found that their impact on SA 0 is not significant ($p > 0.05$) even though there is a difference at the highest level between real-life and remote driving.

2) Safety Assessment: The results of the safety assessment (SA 10) are shown in Fig. 5(b), which shows a trend similar to the overall assessment. In both real-life and remote driving, NF receives the minimal rating, indicating a sense of insecurity among drivers in the absence of SFF. Additionally, the perceived safety during remote driving is also low, potentially caused by various factors in remote driving such as limited visual awareness and the absence of motion feedback. The steering feedback support in SA 11 is in line with the above statement concerning SA 10 (Fig. 5(c)), where NF gives the least support to drivers in both driving conditions.

3) Steering Characteristic Feel: The results of the steering characteristic feel are presented in Fig. 5(d)–(f). For question SA 20 (steering wheel characteristic feel - Fig. 5(d)), the scores in remote driving are almost the same as those for real-life driving. NF is consistently rated lower by the drivers in comparison to other steering feedback models, with a significant difference ($p < 0.01$). However, the difference between PF and MF is not significant ($p > 0.05$). Similarly, the trend shown by the steering feedback force feeling (SA 21) (Fig. 5(e)) is similar to SA 20, but there are significant differences between remote and real-life driving for PF and MF. As indicated by the figure, when the SFF is either PF or MF, drivers can experience an increased steering force in remote driving compared to real-life driving ($p < 0.05$). The average rating of SA 21 for real-life driving is near 2.5, whereas it increases to 3.2 for remote driving. This signifies that the suitable force level for real-life driving appears slightly high for remote driving. This could possibly be caused

by the decreased sensation of steering feedback force in real-life driving due to external environmental disturbances. Conversely, the quiet driving condition of remote driving affords a more distinct perception of steering feedback force. This demonstrates that the requirements for the level of feedback force in remote driving differ from real-life driving and can be tuned to lower levels. As far as steering returnability is concerned, similar patterns with SA 21 are identified (Fig. 5(f)). However, the difference between real-life and remote driving is not significant ($p > 0.05$).

4) Confidence and Control: For confidence and control, NF provides the lowest confidence to drivers in both remote and real-life driving ($p < 0.05$) as presented in Fig. 5(g). PF enhanced drivers' confidence in remote driving in comparison to MF and NF ($p < 0.05$), although the difference between PF and MF is not significant in real-life driving scenarios. As observed in Fig. 5(h), the Level 3 questions regarding confidence and control reveal a marked decline in feeling of success during remote driving compared with real-life driving with PF and MF ($p < 0.05$). On the other hand, the perceived difficulty in remote driving is significantly higher than driving in real-life with PF and MF, as presented in Fig. 5(i). Nevertheless, the difference between the models in remote driving is not significant; this could be due to the fact that the influence of visual or motion feedback might be greater than that of the SFF models.

5) Real-World Feel: Fig. 5(j)–(l) depict the results related to the real-world feel for questions SA 40 - 42. As shown in Fig. 5(j), MF provides remote drivers with a significantly better real-world feel ($p < 0.01$) compared to PF and NF during remote driving, which is in line with disturbance feel in Fig. 5(k). To explore how the real-world feel is affected, a correlation analysis between these subjective assessments (SAs) is performed, as illustrated in Fig. 6(a) and (b).

In these heatmap matrixes, the deeper colours and larger diameter circles represent a higher correlation coefficient between the two SAs. The values of the coefficients are also displayed within each circle. Based on these figures (Fig. 6(a) and (b)), the coefficient between disturbance feel (SA 41) and real-world feel (SA 40) is 0.64 in real-life driving and 0.95 in remote driving. The linear regression analyses between them are also illustrated in Fig. 6(c) and (d), respectively. These correlation levels show that the disturbance feel during remote driving could give remote drivers a strong real-world feel. However, this effect would be reduced in real-life driving. This is probably because the drivers would feel the disturbance through other feedback channels (e.g., chassis, suspension, etc.) during real-life driving, which could partially cover the feel of vibrations from the steering wheel. For the correlation between SA 40 and SA 42, both have high coefficients in real-life and remote driving, which might be because these two questions have the similar meaning, such as real-world feel and realistic feel. Thus, drivers tend to assess them similarly, which leads to a high correlation between them. There are also similar correlations between SA 41 and SA 42, and SA 41 and SA 40, indicating that one of the questions is redundant between SA 40 and SA 42, and it could be avoided in a future experiment.

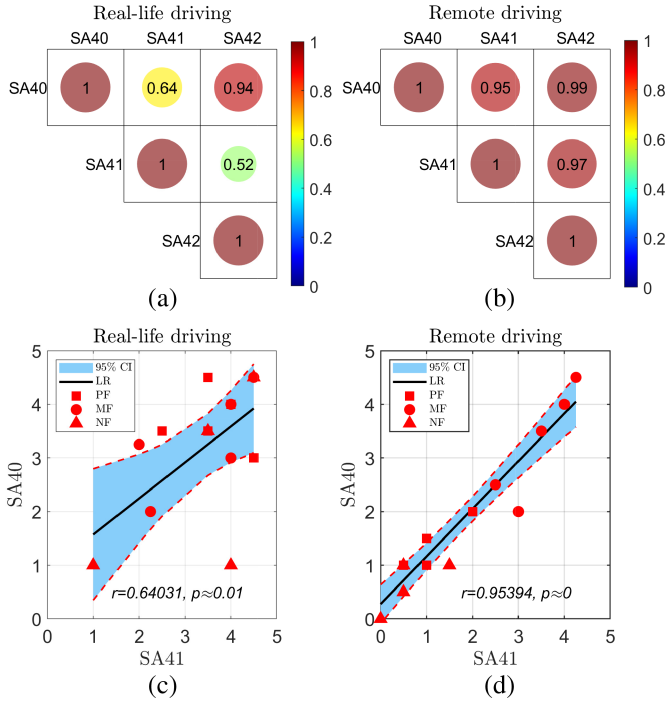

Fig. 6. (a) Correlation matrix between SA 40, SA41, and SA 42 in real-life driving. The value within each circle represents the coefficient between the two SAs. (b) Correlation matrix in remote driving. (c) Linear regression between SA 41 and SA 40 in real-life driving. (d) Linear regression between SA 41 and SA 40 in remote driving. (*CI: Confidence Interval; LR: Linear Regression.*).

6) Summary of Survey Results: The survey results in terms of the four themes mentioned in Section IV are summarized in this section. Concerning the difference in steering feedback between remote and real-life driving (*Theme a*), remote drivers feel that there is less realism and connection to the road. This is because they do not receive the vibrations transmitted by the chassis that conventional drivers feel. When discussing essential characteristics to enhance driving performance (*Theme b*), drivers provide suggestions in various areas, such as lower latency, higher frequency vibration feedback, and better speed awareness. Regarding potential enhancements in steering feedback for remote driving (*Theme c*), drivers believe that a better real-world feel is needed. Also, they state that the level of steering feedback force should be reduced, matching the SA 21 results (Fig. 5(e)). This signifies that they need less steering feedback force during remote driving, potentially due to the changed driving environment. For difficulties in remote driving (*Theme d*), drivers report that the visibility become worse, and it is hard to judge distance and position. In addition, there are also other types of disadvantages, such as less physical reality, less speed awareness, and an unsafe feeling. Multiple factors (such as poorer visibility and no motion cues compared to real-life driving) could have influenced these.

The more detailed comments of each participants can be found in [42]. The comments from this survey indicate the possible challenges facing remote driving and thus pave the way for future

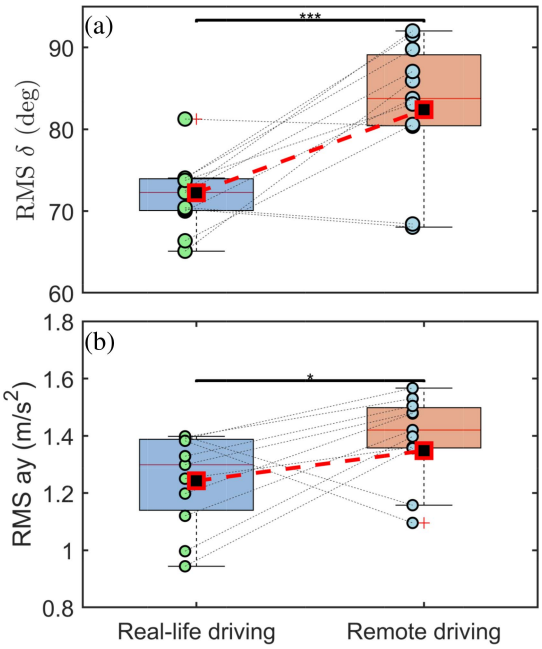

Fig. 7. (a) RMS value of steering angle input (δ) during slalom. (b) RMS value of lateral acceleration (ay) during slalom.

research, such as improving situational awareness, providing more realistic driving feedback, and overcoming latency.

C. Driving Behavior Analysis

1) Driving Behavior in Slalom: In this study, lateral and longitudinal driving behavior and the vehicle's dynamic response are investigated for both real-life and remote driving. Furthermore, the ANOVA and Effect size analysis are employed to analyze the influence of SFF models on driving behavior and performance, specifically focusing on lateral control and lane following.

Driving behavior in lateral control: The metric of steering angle input (δ) is used for analysing the change in driving behaviour, in conjunction with the lateral dynamics of the vehicle, represented by lateral acceleration (ay). To elaborate, the root-mean-square (RMS) values of these variables, namely the δ and ay, are computed.

The point-to-point analysis method is used to explore in detail the changes in driving behavior during remote driving. As depicted in Fig. 7(a), there is a significant trend that remote drivers would provide larger steering angle ($p < 0.001$). Albeit the number of participants is limited, there is high consistency between the data. The underlying cause for the larger steering angle is probably that drivers in RDS have less situational awareness regarding distances, speed, and vehicle motion states. This makes it more difficult for them to continuously and accurately approximate the position of the physical objects, which can account for potential deviations. Therefore, drivers eventually make larger adjustments to correct the vehicle's path.

These changed driving behaviors would also cause changes in the vehicle's dynamic responses, such as lateral acceleration (Fig. 7(b)). The overall lateral acceleration of remote driving is higher compared to driving in real life ($p = 0.027$), which is in line with the steering angle input data (Fig. 7(a)). The increased lateral acceleration could potentially cause the participants' discomfort, while from a safety perspective, the vehicle could become unstable during extreme manoeuvres, such as when avoiding obstacles or driving on low adhesion coefficient roads. An advanced driver assistance system (ADAS) would probably be required to increase remote driving safety for the remote driver.

Regarding the influence of SFF models on steering angle input and lateral acceleration response, no significant effect is found. For the steering angle input, the results of the ANOVA and Effect size for real-life driving are $F(2, 12) = 0.6, p = 0.57, \eta^2 = 0.09$, and for remote driving, $F(2, 12) = 0.32, p = 0.73, \eta^2 = 0.05$. For vehicle lateral acceleration, the statistical results for real-life and remote driving are $F(2, 12) = 0.23, p = 0.80, \eta^2 = 0.04$ and $F(2, 12) = 0.08, p = 0.93, \eta^2 = 0.01$, respectively. It indicates that the SFF models do not significantly influence the steering angle input and vehicle lateral acceleration response in both these cases.

Driving behavior in longitudinal control: Throttle reversal rate (TRR) is a metric that can reflect the tuning frequency of the throttle pedal during driving. A higher TRR means that drivers use pedals with higher frequency to control the speed, indicating that they are modulating the speed more. The method of calculating TRR bears resemblance to the procedure for calculating the Steering Reversal Rate (SRR) as detailed in [43]. For the purposes of this study, the TRR gap is designated as 5 %, implying an increment in TRR value for every alteration in the throttle pedal exceeding 5 %. Prior to TRR computation, the throttle engagement data is filtered through a 10 Hz low-pass filter.

As evidenced by Fig. 8(a), the TRR observed in remote driving is lower in comparison with real-life driving ($p = 0.0349$). It indicates that drivers tune the speed at a lower frequency and keep the throttle in a more static position. This is probably due to their low speed awareness in RDS, where they rely mainly on video and audio to judge speed and distance. On the other hand, in real-life driving, participants have a better sensation of speed through sound, vibrations, and the actual real-life view, as well as the headwind experienced while in the RDV. This could probably provide them with increased awareness to control the speed with the throttle pedal.

In addition to the TRR, the driving speed is presented in Fig. 8(b). The speed is normalised using (13)

$$v_{\text{norm}} = \frac{v - v_{\min}}{v_{\max} - v_{\min}} \tag{13}$$

where v_{norm} represents the normalized velocity, with v denoting the vehicle velocity, while $v_{\min}$ and $v_{\max}$ correspond to the minimum and maximum velocities recorded for each drive, respectively. The findings indicate that it is easy for remote drivers to maintain a low velocity compared to real-life driving, with a p-value of 0.0066. This tendency to reduce speed is probably attributable to more cautious driving behavior at the remote driving station due to the limited feedback information.

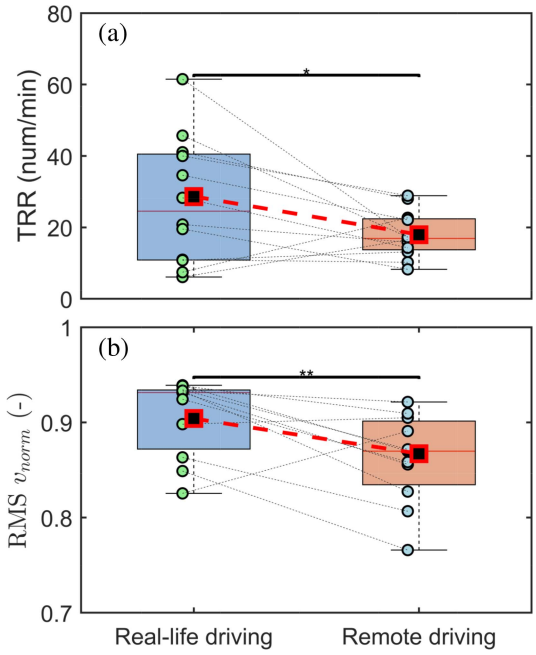

Fig. 8. (a) TRR during slalom. (b) Normalized velocity during slalom.

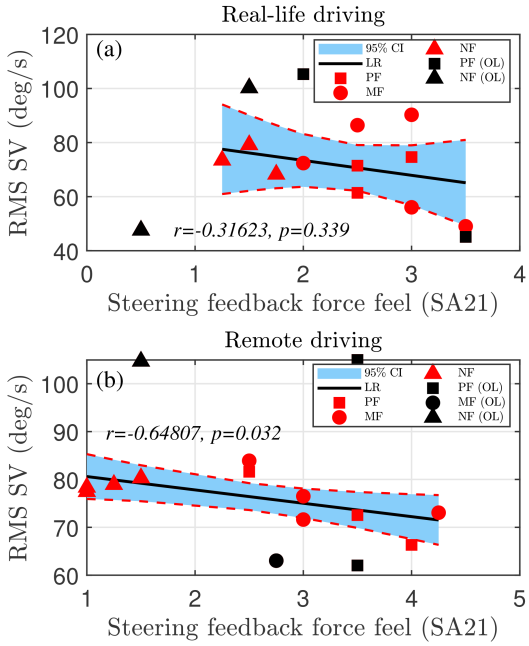

Fig. 10. Correlation between the amplitude of the steering feedback force feel and SV. (a) Real-life driving. (b) Remote driving. (*OL: Outlier; CI: Confidence Interval; LR: Linear Regression*).

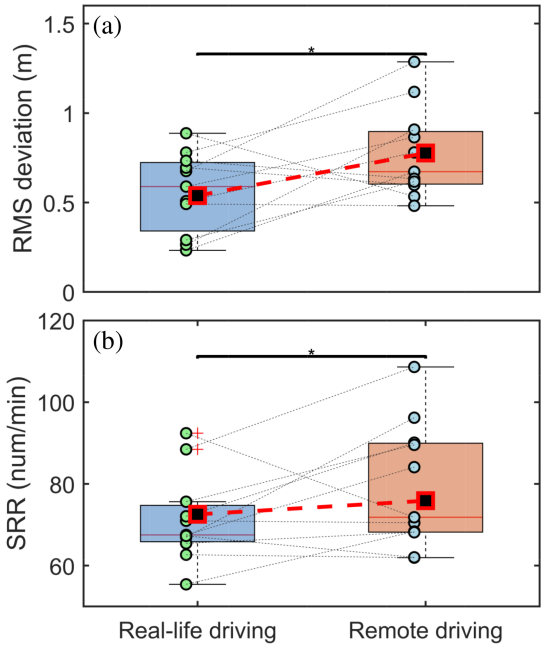

Fig. 9. (a) Lane following deviation. (b) SRR during the lane following manoeuvre.

2) Driving Performance and Behavior in Lane Following Manoeuvre: The RMS value of lane following deviation is calculated to evaluate driving performance. Fig. 9(a) shows the differences in driving performance between remote and real-life driving. The data reveals that the deviation in lane following is significantly bigger in remote driving as compared to real-life driving, with a significance level of $p = 0.0244$. Such discrepancies may arise from various factors, e.g. poor view and absence of motion cues, in the remote driving station.

For the lane-following manoeuvre, the SRR metric is computed, selecting a gap size of 1 degree and establishing a cut-off frequency at 2 Hz. The findings, depicted in Fig. 9(b), indicate that the SRR in remote driving is significantly higher compared to real-life driving ($p = 0.0474$). This suggests a higher frequency of steering corrections by remote drivers, potentially attributed to factors akin to those leading to increased lane following deviation in remote driving. The challenge of approximating the distance will increase through the monitor, which requires them to correct their steering more frequently in order to keep the front-left tyre following the lane.

In addition, the ANOVA and Effect size calculation show a similar result with that in slalom scenario. For lane following deviation, the results are $F(2, 12) = 0.09, p = 0.92, \eta^2 = 0.01$ and $F(2, 12) = 0.33, p = 0.73, \eta^2 = 0.05$ for real-life and remote driving, respectively. For the SRR, the statistical results are $F(2, 12) = 1.1, p = 0.36, \eta^2 = 0.15$ and $F(2, 12) = 1.23, p = 0.32, \eta^2 = 0.17$, respectively. These statistical results indicate that the SFF models also do not have significant influence on lane following deviation and SRR during the lane following manoeuvre. A more detailed analysis of this aspect can be found in the author's previous study [22].

D. Correlation Between Driving Behavior and Experience

A correlation analysis is performed between the steering feedback force feel and the amplitude of steering velocity (SV) during the lane following manoeuvre (Fig. 10(a) and (b)). In remote driving, there is a correlation between them ($r = -0.648, p = 0.032$) as presented in Fig. 10(b). However, the correlation is

weak in real-life driving ($r = -0.3162, p = 0.339$), although the trend is similar to that for remote driving (Fig. 10(a)). According to Fig. 10, drivers with NF have less steering feedback force feel and tend to give a higher steering velocity, which is easier due to the lack of resistance force from the steering wheel. In contrast, with MF and PF, remote drivers would feel a higher steering feedback force and give a lower steering velocity. Therefore, this correlation indicates that the amplitude of the steering feedback force could affect steering velocity in remote driving. However, there are some other feedback channels that could influence the steering velocity in real-life driving, such as motion-cueing. Therefore, the influence of the amplitude of the steering feedback force feel on steering velocity could be mitigated. This could probably be the reason why no significant correlation is found between them in real-life driving as presented in Fig. 10(a).

VI. Conclusion

This article presents a comparative analysis focusing on the distinctions in driving behavior and experience between remote and real-life driving. Concurrently, the physical and modular model-based steering force feedback has been developed to investigate the requirements of SFF for remote drivers. The subjective assessment questionnaire, encompassing questions ranging from general to specific, has been created to evaluate the effect of SFF on the driving experience. The main conclusions in terms of research aims are summarised as follows:

- In the conducted experiment, participants are able to adapt to a specific scenario following four iterations of practice in both remote and real-life driving contexts (*RA1*).
- In remote driving, the required amplitude of feedback force and returnability is observed to be less compared to real-life driving, which could be caused by the alterations in the driving environment experienced in remote driving. In addition, the road disturbance feel through the steering wheel would have a higher correlation with the real-world feel for drivers during remote driving than that for real-life drivers. This implies that the requirements of SFF model in remote driving might vary from those in real-life driving, indicating that the corresponding standards related to steering force feedback modelling should be reconsidered for remote driving (*RA2*).
- Remote drivers tend to feel unsafe and think that remote driving is more difficult than real-life driving. Moreover, the driving experience appears to worsen when there is no steering force feedback during both real-life and remote driving. Drivers do not feel much difference between the PF and MF. However, MF could provide a more realistic feeling during remote driving due to the disturbance information provided by the steering motor current. This indicates that a suitable SFF is necessary for providing a good driving experience, and the realistic feeling could be improved if suitable road disturbances can be transmitted (*RA3*).
- For the driving behavior analysis, this paper focuses on comparing the differences between real-life and remote driving by combining the data of three SFF models together. It is found that the drivers tend to provide larger and faster steering angle inputs in the slalom manoeuvre during remote driving, which could probably increase the possibility of vehicle instability and passenger discomfort. Furthermore, it is easy for the drivers to keep a lower speed, and the TRR would also decrease during remote driving in this manoeuvre. The lane following performance also becomes worse compared with real-life driving. This signifies that the overall driving performance in this remote driving experiment will be worse even with steering force feedback, and some remote driving assisted system could possibly be used to improve this. In addition, no significant impact of SFF models on driving behavior and performance is observed in the context of vehicle lateral control and lane following, for either real-life or remote driving (*RA4*).
- In this remote driving experiment, the amplitude of the steering feedback force has a negative correlation with the steering velocity of remote drivers. This suggests that the driving experience might potentially affect the behavior of remote drivers. Therefore, providing appropriate driving feedback becomes crucial to enhance both the driving experience and behavior (*RA5*).

Limitations of the study: There are three main limitations in this study. First, the remote driving platform's communications use only one simcard. There is a possibility to provide more stable signal transmission using dual carriers. Second, there is further room to improve the visual and auditory feedback by using more advanced camera, screen, and surrounding microphone techniques. Third, the participant pool is constrained in number, although each participant performs each driving manoeuvre three times and the objective metrics are highly consistent. Therefore, a future study could be done based on the following two aspects: first, recruiting a more diverse group of participants with respect to age, gender, and driving experience, and second, employing more advanced remote driving technologies.

Acknowledgment

Gratitude is extended towards the contributors who financially support this research. Furthermore, valuable support is also received from TRENoP. Ethical Approval: The study receives approval from the Swedish Ethical Review Authority (Ref no.: 2020-05020). Informed consents are duly obtained from all participants.

References

[1] P. Ghorai, A. Eskandarian, Y. K. Kim, and G. Mehr, "State estimation and motion prediction of vehicles and vulnerable road users for cooperative autonomous driving: A survey," *IEEE Trans. Intell. Transp. Syst.*, vol. 23, no. 10, pp. 16983–17002, Oct. 2022.

[2] L. Chen et al., "Milestones in autonomous driving and intelligent vehicles: Survey of surveys," *IEEE Trans. Intell. Veh.*, vol. 8, no. 2, pp. 1046–1056, Feb. 2023.

[3] K. Wang, T. Zhou, X. Li, and F. Ren, "Performance and challenges of 3D object detection methods in complex scenes for autonomous driving," *IEEE Trans. Intell. Veh.*, vol. 8, no. 2, pp. 1699–1716, Feb. 2023.

[4] "Waytous," 2022. [Online]. Available: https://cathayinnovation.com/company/waytous/

[5] "Einride will hire remote truck driver in 2020," 2020. [Online]. Available: https://www.einride.tech/insights/einride-will-hire-its-first-remote-autonomous-truck
[6] "Vay," 2022. [Online]. Available: https://vay.io/
[7] J. M. Georg and F. Diermeyer, "An adaptable and immersive real time interface for resolving system limitations of automated vehicles with teleoperation," in *Proc. IEEE Int. Conf. Syst. Man Cybern.*, 2019, pp. 2659–2664.
[8] X. Ge, M. J. Brudnak, P. Jayakumar, J. L. Stein, and T. Ersal, "A model-free predictor framework for tele-operated vehicles," in *Proc. IEEE Amer. Control Conf.*, 2015, pp. 4573–4578.
[9] M. R. Endsley, "Design and evaluation for situation awareness enhancement," in *Proc. Hum. Factors Soc. Annu. Meeting*, vol. 32, no. 2, pp. 97–101, 1988.
[10] L. Zhao, M. Nybacka, and M. Rothhämel, "A survey of teleoperation: Driving feedback," in *Proc. IEEE Intell. Veh. Symp. (IV)*, 2023, pp. 1–8.
[11] T. Tang, J. Kurkowski, and M. Lienkamp, "Teleoperated road vehicles: A novel study on the effect of blur on speed perception," *Int. J. Adv. Robot. Syst.*, vol. 10, no. 9, pp. 333–344, Sep. 2013.
[12] S. Neumeier, P. Wintersberger, A. K. Frison, A. Becher, C. Facchi, and A. Riener, "Teleoperation: The holy grail to solve problems of automated driving? sure, but latency matters," in *Proc. 11th Int. Conf. Automot. User Interfaces Interactive Veh. Appl.*, 2019, pp. 186–197.
[13] S. Lu, M. Y. Zhang, T. Ersal, and X. J. Yang, "Workload management in teleoperation of unmanned ground vehicles: Effects of a delay compensation aid on human operators' workload and teleoperation performance," *Int. J. Hum–Comput. Interact.*, vol. 35, no. 19, pp. 1820–1830, Nov. 2019.
[14] E. Nakamura, "Signal time-delay tolerance in teleoperated vehicles," in *Proc. IEEE 10th Glob. Conf. Consum. Electron.*, 2021, pp. 770–773.
[15] S. Vozar and D. M. Tilbury, "Improving UGV teleoperation performance using novel visualization techniques and manual interfaces," in *Proc. SPIE 8387 Unmanned Syst. Technol. XIV*, 2012, pp. 838716(1)–838716(8).
[16] D. R. Tyczka, R. Wright, B. Janiszewski, M. J. Chatten, T. A. Bowen, and B. Skibba, "Study of high-definition and stereoscopic head-aimed vision for improved teleoperation of an unmanned ground vehicle," in *Proc. SPIE Unmanned Syst. Technol. XIV*, 2012, pp. 83870L(1)–83870L(18).
[17] A. Tandon, M. J. Brudnak, J. L. Stein, and T. Ersal, "An observer based framework to improve fidelity in internet-distributed hardware-in-the-loop simulations," in *Proc. ASME Dyn. Syst. Control Conf.*, 2014, pp. 1–9.
[18] Y. Zheng, M. J. Brudnak, P. E. A. Jayakumar, J. L. Stein, and T. Ersal, "Evaluation of a predictor-based framework in high-speed teleoperated military UGVs," *IEEE Trans. Hum.-Mach. Syst.*, vol. 50, no. 6, pp. 561–572, Dec. 2020.
[19] G. Graf, H. Xu, D. Schitz, and X. Xu, "Improving the prediction accuracy of predictive displays for teleoperated autonomous vehicles," in *Proc. IEEE 6th Int. Conf. Control Automat. Robot.*, 2020, pp. 440–445.
[20] J. Prakash, M. Vignati, S. Arrigoni, M. Bersani, and S. Mentasti, "Teleoperated vehicle-perspective predictive display accounting for network time delays," in *Proc. ASME*, 2019, pp. 1–9.
[21] G. Papaioannou, L. Zhao, M. Nybacka, J. Jerrelind, R. Happee, and L. Drugge, "Motion comfort and driver feel: An explorative study about their relation in remote driving," 2023, *arXiv:2305.07370*.
[22] L. Zhao et al., "Study of different steering feedback models influence during remote driving," in *Advances in Dynamics of Vehicles on Roads and Tracks*. Berlin, Germany: Springer, 2021, pp. 836–853.
[23] D. Lee, K. Yi, S. Chang, B. Lee, and B. Jang, "Robust steering-assist torque control of electric-power-assisted-steering systems for target steering wheel torque tracking," *Mechatronics*, vol. 49, pp. 157–167, Feb. 2018.
[24] J. Lee, K. Yi, D. Lee, B. Jang, M. Kim, and S. Hwang, "Haptic control of steer-by-wire systems for tracking of target steering feedback torque," *Proc. Inst. Mech. Engineers Part D: J. Automobile Eng.*, vol. 234, no. 5, pp. 1389–1401, Apr. 2020.
[25] M. Goodrich and M. Quigley, "Learning haptic feedback for guiding driver behavior," in *Proc. IEEE Int. Conf. Syst., Man Cybern.*, 2004, pp. 2507–2512.
[26] K. T. R. V. Ende, D. Schaare, J. Kaste, F. Küçükay, R. Henze, and F. K. Kallmeyer, "Practicability study on the suitability of artificial, neural networks for the approximation of unknown steering torques," *Veh. Syst. Dyn.*, vol. 54, no. 10, pp. 1362–1383, Oct. 2016.
[27] A. Balachandran and J. C. Gerdes, "Designing steering feel for steer-by-wire vehicles using objective measures," *IEEE/ASME Trans. Mechatron.*, vol. 20, no. 1, pp. 373–383, Feb. 2015.
[28] Y. Jiang, W. Deng, J. Wu, S. Zhang, and H. Jiang, "Adaptive steering feedback torque design and control for driver–vehicle system considering driver handling properties," *IEEE Trans. Veh. Technol.*, vol. 68, no. 6, pp. 5391–5406, Jun. 2019.
[29] D. Toffin, G. Reymond, A. Kemeny, and J. Droulez, "Role of steering wheel feedback on driver performance: Driving simulator and modeling analysis," *Veh. Syst. Dyn.*, vol. 45, no. 4, pp. 375–388, Apr. 2007.
[30] B. Shyrokau, J. Loof, O. Stroosma, M. Wang, and R. Happee, "Effect of steering model fidelity on subjective evaluation of truck steering feel," in *Proc. Driving Simul. Conf. Exhib.*, 2015, pp. 39–46.
[31] S. Fankem and S. Müller, "A new model to compute the desired steering torque for steer-by-wire vehicles and driving simulators," *Veh. Syst. Dyn.*, vol. 52, no. sup1, pp. 251–271, May 2014.
[32] B. H. Nguyen and J. H. Ryu, "Direct current measurement based steer-by-wire systems for realistic driving feeling," in *Proc. IEEE Int. Symp. Ind. Electron.*, 2009, pp. 1023–1028.
[33] G. L. Gil Gómez, M. Nybacka, E. Bakker, and L. Drugge, "Objective metrics for vehicle handling and steering and their correlations with subjective assessments," *Int. J. Automot. Technol.*, vol. 17, no. 5, pp. 777–794, Oct. 2016.
[34] Y. J. Woo and J. Giacomin, "The role of the scale and the frequency bandwidth of steering wheel vibration on road surface recognition," in *Proc. 8th Int. Symp. Adv. Veh. Control*, , 2006.
[35] W. H. Chen, J. Yang, L. Guo, and S. H. Li, "Disturbance-observer-based control and related methods'an overview," *IEEE Trans. Ind. Electron.*, vol. 63, no. 2, pp. 1083–1095, Feb. 2016.
[36] U. Mandhata, J. Wagner, F. Switzer, D. Dawson, and J. Summers, "A customizable steer-by-wire interface for ground vehicles," *IFAC Proc. Volumes*, vol. 43, no. 7, pp. 656–661, Jul. 2010.
[37] E. Bakker, L. Nyborg, and H. B. Pacejka, *Tyre Modelling for Use in Veh. Dyn. Stud.*, Warrendale, PA, USA: SAE, 1987.
[38] "Using pacejka 89 and 94 models," 2005. [Online]. Available: https://vdocuments.mx/reader/full/using-pacejka-89-and-94-models
[39] J. W. Wang, H. Wang, C. H. Jiang, Z. W. Cao, Z. H. Man, and L. Chen, "Steering feel design for steer-by-wire system on electric vehicles," in *Proc. IEEE Chin. Control Conf.*, 2019, pp. 533–538.
[40] U. B. Mandhata, M. J. Jensen, J. R. Wagner, F. S. Switzer, D. M. Dawson, and J. D. Summers, "Evaluation of a customizable haptic feedback system for ground vehicle steer-by-wire interfaces," in *Proc. IEEE Amer. Control Conf.*, 2012, pp. 2781–2787.
[41] H. Liao, Y. Li, and G. Brooks, "Outlier impact and accommodation methods: Multiple comparisons of type I error rates," *J. Modern Appl. Stat. Methods*, vol. 15, no. 1, pp. 452–471, May 2016.
[42] L. Zhao, "Teleoperation and the influence of driving feedback on drivers behaviour and experience," Licentiate Thesis, Dept. Eng. Mechanics, KTH Roy. Inst. Technol., 2023. [Online]. Available: https://www.diva-portal.org/smash/record.jsf?pid=diva2%3A1754796&dswid=-1136
[43] G. Markkula and J. Engstroem, "A steering wheel reversal rate metric for assessing effects of visual and cognitive secondary task load," in *Proc. 13th ITS World Congr.*, 2006, pp. 1–12.

Lin Zhao was born in Hebei, China. He received the M.Sc. degree in automotive engineering from Chongqing University, Chongqing, China, in 2019. He is currently working toward the Ph.D. degree with the Department of Engineering Mechanics, School of Engineering Sciences, KTH Royal Institute of Technology, Stockholm, Sweden. From 2017 to 2018, he was a Visiting Student with the State Key Laboratory of Automotive Safety and Energy, Tsinghua University, Beijing, China. From 2019 to 2020, he was a Research Engineer with the Intelligent Vehicle R&D Center of Geely Automobile. His research interests include teleoperation, automated vehicles, human factors, vehicle system dynamics and control, driving simulator control, steering dynamics, and dynamic game theory.

Mikael Nybacka received the Mechanical Engineering degree from the Luleå University of Technology, Luleå, Sweden, in 2005. He also received the Ph.D. degree from Luleå University of Technology. He is currently with the KTH Royal Institute of Technology, Stockholm, Sweden, as an Associate Professor in vehicle dynamics. His research interests include vehicle validation and driver vehicle interaction and also various aspects concerning over-actuated vehicles, the design of over-actuation and urban vehicle concepts, control of automated vehicles, and fault-tolerant control.

Malte Rothhämel was born in Stuttgart, Germany. He received the Dipl. Ing. degree in automotive engineering from Technical University Dresden, Dresden, Germany, in 2006 and the Ph.D. degree from the KTH Royal Institute of Technology, Stockholm, Sweden, in 2013. He is currently an Assistant Professor with the Department of Engineering Mechanics, School of Engineering Sciences, KTH Royal Institute of Technology. From 2014 to 2016, he was the Guest Researcher with Volkswagen Global Research, Wolfsburg, Germany. From 2017 to 2020, he developed fail-operational chassis systems and E/E-architecture for driver-controlled and automated heavy trucks with Scania R&D. His research interests include steering feel, automated vehicles, human factors, vehicle system dynamics, and rolling resistance and comfort.

Azra Habibovic received the Ph.D. degree in vehicle safety systems in 2012 and the M.Sc. degree in electrical and electronics engineering in 2006, both from the Chalmers University of Technology, Gothenburg, Sweden. She is currently the technology Leader for human factors and automation with Scania CV, where she is responsible for defining and driving forward Scania's roadmap for early stage research in these two fields. Prior to joining Scania, Azra was with RISE Research Institutes of Sweden as a Senior Researcher and project Leader, and with the research center SAFER as a research area Director for road user behavior. Her research focuses on improving traffic safety and user experience by means of automation and connectivity. Of special interest to her is the design and evaluation of interactions in and around automated vehicles, including interactions related to remote operation of automated vehicles.

Georgios Papaioannou received the Ph.D. degree from the National Technical University of Athens, Athens, Greece, in 2019, which received an award regarding its innovation and impact. He is currently an Assistant Professor on motion comfort in AVs with TU Delft, Delft, The Netherlands, after conducting postdoctoral research with KTH Royal Institute of Technology, Stockholm, Sweden and Cranfield University, Cranfield, U.K. His research interests include motion comfort, seat comfort, postural stability, human body modelling, automated vehicles, motion planning, optimisation and control.

Lars Drugge received the M.Sc. degree in mechanical engineering in 1994 and the Ph.D. degree in computer aided design in 2000 from the Luleå University of Technology, Luleå, Sweden. He is currently an Associate Professor in vehicle dynamics with the Department of Engineering Mechanics, School of Engineering Sciences, KTH Royal Institute of Technology, Stockholm, Sweden. Assoc. Prof. Drugge is the head of the vehicle dynamics, Rail Vehicles and Conceptual Vehicle Design group. His research interests include vehicle dynamics of over-actuated vehicles, tyre modelling, driver vehicle interaction, and driving simulators.